ISBN: 978-93-94570-00-9

6. One Step Combustion Method for The Preparation of 3n Pure (99.9%) Nano Alumina Powder for Substrate Making in Led Applications

Priyanka Nayar, Pooja Yadav, Paresh Nageshwar

Jawaharlal Nehru Aluminum Research Design and Development Centre, Wadi, Nagpur, Maharashtra, India.

Upendra Singh, Anupam Agnihotri

Jawaharlal Nehru Aluminum Research Design and Development Centre, Wadi, Nagpur, Maharashtra, India.

Abstract:

Alumina (Al_2O_3) is widely used in a variety of applications, because it has superior physical and chemical properties which is high heat resistance, excellent electrical isolation, abrasion resistance and high corrosion resistance. Generally, alumina is manufactured with a purity of 99.6 – 99.9% mainly by the Bayer process with bauxite as the starting material. It is used in refractory products; spark plugs and IC substrate and so on. High purity alumina, which has a purity of more than 99.99% and has a uniform fine particle has been widely used in translucent tubes for high-pressure sodium lamps, single crystal materials such as sapphires for watch covers, high-strength ceramic tools, abrasives for magnetic tape and the like. In recent years, the demand of high purity alumina is expanding in fields which are expected to show a high growth rate e.g., display materials, energy, automobiles, semiconductors and computers. In this paper we report the preparation of Nano-alpha alumina powders with a purity of 3N (99.9%) by two different chemical routes viz. auto combustion and alkoxide methods. XRD, BET surface area, SEM and ICP, TGA, LIBS were used to characterize the powders produced.

Keywords:

Nanomaterials, alumina, auto combustion, alkoxide route, SEM, ICP, XRD.

6.1 Introduction:

The natural sapphire is corundum (α-alumina) with traces of metallic elements that can impart a variety of colors including that found in the familiar blue sapphire (iron & titanium) and ruby (chromium). Production of synthetic sapphire has been possible for over a century (Verneuil, 1902 and Czochralski, 1916) but even as recently as a decade ago, annual world production was only a few hundred tones. The last decade has seen rapid growth in both production and new applications for synthetic sapphire based on a number of fundamental properties of corundum including its high electrical insulating and thermal conductivity properties and its well-known hardness of 9.0 on the Mohs scale. The starting material for

the production of synthetic sapphire is high purity alumina (HPA) which is usually accepted to be greater than or equal to 99.99% purity (4N or 100ppm impurities).

Al_2O_3 or alumina generally refers to corundum. It is a white oxide. Alumina has several phases such as gamma, delta, theta, and alpha. However, the alpha alumina phase is the most thermodynamically stable phase. Al_2O_3 in its α-phase is used as a good ceramic material which has many interesting properties, for example high hardness, high stability, high insulation, and transparency [1]. Alumina is also widely used in the fire retard, catalyst, insulator, surface protective coating, and composite materials [2-6].

Generally, Bayer's process is used for preparing the α-Al_2O_3 [7]. Alumina powder is available abundantly and at a low cost, hence it is a widely used material for making structural components, electronic devices, and substrates etc. There are several other methods of preparation of α-Al_2O_3 like pyrolysis [8], plasma evaporation process [9], sol-gel process [10], molten salt [11], hydrothermal [12], and solvothermal [13] techniques and so on.

These days, nano-sized alumina has attracted much attention due to large surface area in their nano-scale range rather than micron size. It has more applications in nano-matching and nano-probes [14]. The nano-size transition alumina [15] are used to obtain high-quality ceramics. The ceramics are used for the high temperature applications, drug delivery [16], absorbents, and soft abrasive coatings [17] applications. There are several other applications like, thin film or as a dielectric layer in electronic component industry, antireflective coatings [18], refractory, wave-guide sensors [19] and buffer layer [20] etc. It is also being used as nanoparticles in catalysis, as membranes and structural materials.

There are different phases of alumina such as:

- Cubic-spinel
- Tetragonal
- Monoclinic
- Cubic-spinel, and
- Alumina (orthorhombic) [21,22] and α-alumina.

From all the existing phases α-alumina, also called as corundum, is very common and thermodynamically stable [23]. Nano-size alumina is prepared by several techniques like sol gel [24], arc plasma [25] and re-condensation [26] etc. The most popular technique to make ultra-fine Al_2O_3 is sol-gel auto combustion and alkoxide routes because they are low-cost, low pollution and easy to be prepared on large scale.

In some of the previous work done on the preparation of alumina nano-particles is reported by different routes like micro-emulsions [27], microwave [28], sol-gel [29,30], hydrothermal [31-32], but there is no study reported on comparison of the phase transformed nano-particles due to variation in preparation conditions. The different intermediate phases of Al_2O_3 are very unstable and they can be converted to the most stable α-phase by controlling the heat treatment given through the combustion temperature or by increasing the annealing temperature.

In this work more emphasis is given on the behavioral characteristic based on the phase transformation of nano-alumina by the stated two different preparation methods. It is very difficult to obtain the α-phase of alumina at temperatures below 1000° C, we accepted this challenge and tried to achieve it in this course of work.

6.2 Experimental:

6.2.1 Sol Gel Auto Combustion Synthesis:

In this method alumina was prepared by combustion, using metal nitrates as oxidizer and urea as a fuel [33,34]. Stoichiometric amount of pure aluminum nitrate nonahydrate (AR Grade, 99.99% purity) and urea were dissolved in distilled water to obtain a solution that was placed in constant stirring position on a hot plate at a temperature of 70-80oC for 4-5 hours.

This resulted in a clear colorless transparent gel. A crucible containing the gel was inserted at 500° C in a preheated furnace. In few minutes the mixtures swell with evolution of gases and finally a flame appears. The flame lasts for about a minute. The crucible is removed from the furnace after the flame extinguishes. The foamy product is crushed to powder and used for further characterization. Following reaction took place for this process:

$$2Al(NO_3)_3 + 5(NH_2)_2CO \xrightarrow{\triangle} Al_2O_3 + 8N_2\uparrow + 5CO_2\uparrow + 10H_2O\uparrow \quad \ldots (1)$$

6.2.2 Alkoxide Route:

During this process, high purity aluminum alkoxide was synthesized from aluminum metal and alcohol, and hydrated alumina was produced by hydrolysis of alkoxide, and finally high purity alumina was formed.

For synthesis of alumina powder, 27 g of low-cost packaging grade aluminum foil was treated with 300 ml of anhydrous isopropyl alcohol (99.99% pure) under reflux, 0.2 gm of iodine was added as a catalyst and 1.6 gm of mercuric chloride dissolved in 40 ml of isopropanol and was released in reflux solution chamber after dissolution. After 1.5 hr excess of IPA was distilled out at 82°C and aluminum isopropoxide was distilled out at 135-140°C in gel form which was automatically dried at room temperature. The following reaction takes place with aluminum foil and isopropanol to form aluminum isopropoxide.

$$Al + 3ROH \xrightarrow{\triangle} Al(OR)_3 + 3H\uparrow \quad \ldots(2)$$

Preparation of aluminum isopropoxide was followed by its hydrolysis to get hydrated alumina. For this, 4 gm of dried aluminum isopropoxide was mixed with 15 ml anhydrous isopropanol and 15 ml distilled water and kept on stirring on a hot plate (70-80oC) for 6-7 hrs in a closed glass container. Sample solution was then filtered using Whatman filter paper. Obtained powder was oven dried (110oC) and then calcined at 1200oC to get pure alumina. Hydrolysis of aluminum isopropoxide was carried out by following reaction:

$$2Al(OR)_3 + 4H_2O \xrightarrow{\Delta} Al_2O_3.H_2O + 6\,OR\downarrow \quad \ldots(3)$$

$$Al_2O_3.H_2O \xrightarrow{\Delta} Al_2O_3 + H_2O \quad \text{(Calcination at 1200°C)} \quad \ldots(4)$$

The as prepared Al_2O_3 powder obtained from both the methods was then crushed manually and taken for characterization as described in the following section.

6.2.3 Characterization:

X-ray diffraction measurements were performed on 3N pure alumina sample prepared by both the techniques (as mentioned above) using the Philips diffractometer in the grazing incidence geometry with Cu-Kα radiations (λ= 1.54056 Å). XRD studies were performed by keeping the incidence angle fixed at 20° and scanning the scintillation detector in the 2ϴ range of 10^o to 70^o.

Impurity analysis of Minor elements present in sample was determined by Inductively Couple Plasma-Optical Emission Spectrometer (ICP); model ICAP-7400 Thermo Fisher Scientific at JNARDDC. Chemical analysis of alumina revealed the nature of minor impurity elements. The method adopted for sample preparation of ICP analysis is acid digestion as described below,

0.5 g of oven dried alumina powder sample was taken in a platinum crucible containing fusion mixture of H_3BO_3 & Na_2CO_3 in 1:3 ratios. Sample was then subjected to heat treatment at 1000^oC in previously heated furnace for about one hour. Fused sample mass was then extracted with 1:1 HCL solution in hot condition & after dissolution & cooling, volume of alumina sample solution was then made up to 250 ml in a volumetric flask using ultra-pure water. Stock solution prepared was then analyzed for trace impurity by using ICP-OES and flame photometer. A blank solution was prepared to ensure any contamination. Table 6.1 gives the analytical methods for chemical characterization of alumina powder:

Table 6.1: Analytical method used for chemical characterization of alumina powder

Component	**Chemical Characterization techniques**
Na_2O	Fusion at 1000^0 C+ HCL extraction of sample in hot condition followed by Flame Photometric analysis
Minor + Trace	Fusion at 1000^0 C+ HCL extraction of sample in hot condition followed by ICP analysis

Surface morphology and homogeneity of the samples were examined using Scanning Electron Microscopy (SEM). Surface area of the prepared powders was easily determined using the Micromeritics ASAP 2020 gas adsorption analyzer and the application of the well-established BET method. AccuPyc II 1345 Pycnometer was used to calculate the density of alumina powder by measuring the amount of displaced helium gas. Thermo Gravimetric Analysis (TGA) was performed on alumina powders in air using a simultaneous thermal analyzer STA 409-PC Luxx in the temperature range between RT-1000°C at a heating rate of 10°C/min to verify the change in weight during conversion of phases at different temperatures. Thermographs provide information regarding the comparison of mass change with temperature for alumina sample.

The purity of the Al_2O_3 powder was analysed by using laser induced breakdown spectroscopy method. The Al_2O_3 pellet was made and the same is subjected to sintering at 1200oC. Finally, laser induced breakdown spectra of Al_2O_3 was recorded with different energy levels such as 5mJ, 10 mJ and 15 mJ respectively.

Al_2O_3 powder was subjected for thermal analysis with different time intervals such as 5, 10, 15, 20, 25 and 30 min. respectively to calculate the thermal conductivity as well as diffusivity.

6.3 Results and Discussion:

The as prepared Al_2O_3 nano-alumina powder was first taken for XRD characterization for confirming the phase formation during the sol-gel auto combustion method. Fig. 1 shows the XRD diffraction pattern taken on Philips X-ray Diffractometer in the grating incidence geometry with Cu- K α radiation (λ=1.54056Å) compared with the standard α-alumina XRD pattern. It shows that there is an excellent match of the X-ray diffraction between both the patterns of lines corresponding to the same crystal structure.

There were no lines found which corresponds to the other phases of nano alumina, this satisfies that only single-phase nano alumina is obtained by the sol-gel auto combustion method at 450°C furnace temperature without any post annealing treatment. The XRD pattern does not changes even if the as prepared alumina powder is kept for annealing at the temperature say, 1000° C. Hence, these results show the formation of highly crystalline material α-alumina with a stable and irreversible phase.

The earlier studies show that nano alumina can be synthesized by SGAC process by initiating exothermic reaction with the mixture of urea + glycine as the fuel for exothermic reaction and produces the crystalline mixed phase [35].

Khorrami et.al. synthesized nano crystalline Al_2O_3 with sol-gel auto combustion and ultrasonic method but obtained γ-Al_2O_3 [36]. In another study it was reported that the complexing agent as citric acid which reduces the formation temperature to 750°C from 1000°C but yields the γ-phase of Al_2O_3 [37]. Roque et. al. prepared nano-alumina powder by combustion synthesis and got the FCC structure of the α-Al_2O_3 because of the excess of urea which restricts the complete oxidation of Al ions [38].

Figure 6.2 below shows the XRD pattern of alumina Nano powders prepared by alkoxide route. It is found that α-alumina was obtained by calcining hydrated alumina at high temperature of 1200^{o}C after the rearrangements of oxygen packing. Ideally α-phase of alumina was obtained after calcination of hydrated alumina via different intermediate phases (γ, δ, θ etc).

Complete phase transition to thermodynamically stable phase of alumina strictly depends on the control of hydrolysis conditions as well as uniformity of temperature distribution during calcination [39]. Different researchers worked in order to lowering the transition temperature as below as 1000^{o}C or even lower either by using seed crystals [40-42], or by adding elemental impurities [43].

On comparing the phase transformation of alumina nanoparticles prepared by sol gel auto combustion and alkoxide routes, it can be concluded that direct fuel combustion is needed to decompose aluminium nitrate with large amount of energy whereas in alkoxide route, calcination temperature of 1200^{o}C is required to obtain α-phase of alumina that too with controlled conditions of hydrolysis, drying and calcination. Therefore, factors such as preparation methodology, precursor selection, annealing/combustion temperature, and time affect the crystallization properties of synthesized nanoparticles.

Figure 6.3 (a) and (b) shows SEM images with surface morphology of alumina nanoparticles prepared by auto combustion and alkoxide process respectively. Micrographs of 3N powder prepared by auto combustion process shows nano agglomerates which resulted in lower surface area whereas alumina formation by alkoxide route resulted in aggregates of crystallites that form network and chain like structure with high surface area and this kind of mesoporous structure could be suitable for various applications i.e. adsorption or catalysis etc.

Table 6.1 and 6.2 below shows the extent of impurities recorded by ICP-OES for the powder obtained by auto combustion and alkoxide route respectively. 3N pure alumina was clearly formed using both routes although minor trace impurities were observed in the one prepared by alkoxide method due to the distillation process used for the purification.

Table 6.2: Chemical Composition of alumina in traces prepared by auto combustion method

Alumina	Composition
Fe_2O_3	**79.51 ppm**
SiO_2	**63.56 ppm**
CaO	**34.72 ppm**
MgO	**37.18 ppm**
Na	**0.028 %**
Al_2O_3 (by diff)	**99.95 %**

Table 6.3: Chemical composition of alumina powder prepared by alkoxide route

Alumina	Composition
Fe_2O_3	**74 ppm**
CaO	**34.5 ppm**
TiO_2	**0.5 ppm**
Al_2O_3 (by diff)	**99.98 %**

TG/DTA analysis of alumina samples generated by both the techniques were done to check thermal stability & change in weight with respect to increase in temperature. Fig. 4 show the TG behavior of alumina prepared via combustion method where negligible mass change was observed. Moisture was lost at 200°C. Endothermic peaks at 400°C and after 600°C were the result of evaporation of bonded water molecules. The overall mass loss for this sample was 1.55 %. Mass loss was found to be 0.92 % if we ignore the mass lost due to moisture. The reduction in mass loss was due to the high temperature generated during Auto combustion.

TG behavior of alumina prepared via alkoxide rout is as presented in Figure 6.5 below. From the thermograph it was found that after annealing alumina sample directly at 1200°C, bonded water molecules got evaporated therefore curve has not shown any mass change or endothermic peak.

Density of both the samples were determined using Helium gas displacement technique. Density values for alumina powder by both the methods are given in Table 6.4.

Table 6.4: Density of alumina powders

Property	Sample Combustion	Sample Alkoxide	Standard
Density (g/cm^3)	3.78	3.88	3.9

Highest density of 3.88 g/cm^3 was achieved for the sample annealed at 1200^{o}C although density values of both the alumina powders were very close to that of standard alumina (3.9 g/cm^3) and found to be within the range of Sumitomo's high purity alumina (3.8-3.9). In order to use the above prepared alumina powder for the substrate making in LED fabrication, some of the characterizations were performed to test the powder for its spectroscopic and thermal properties.

Figure 6.6 shows the laser induced breakdown spectra of Al_2O_3 powder. From the spectra it is observed that along with Al and O, traces of Fe, Ca and Si element were also present in ppm range. Trichard et. al. reported the imaging of alumina support by laser induced breakdown spectra and found that LIBS can provide quantitative concentration including sulphur, vanadium and nickel in the ppm range. The report indicates that LIBS-based imaging represents a powerful tool for quickly providing two-dimensional elemental map over a large dynamic range i.e., typically from ppm to tens of percent [35].

Thermal conductivity and thermal diffusivity of Al_2O_3 powder at different time intervals of 5, 10, 15, 20, 25 and 30 mins are summarised in Table 6.5. The obtained results are in good agreement with previous literature [35]. These low values of conductivity and diffusivity are due to the presence of large number of pores in the powder and the absence of bonding between its particles. Solid alumina has a thermal conductivity 100 times higher than powdered alumina.

Table 6.5: Thermal properties of Al2O3 at different time intervals

Description	Thermal Conductivity (W/mK)	Thermal Diffusivity (mm^2/s)
Al_2O_3 (5 mins)	0.2764	0.2666
Al_2O_3 (10 mins)	0.2039	0.1793
Al_2O_3 (15 mins)	0.2278	0.1749
Al_2O_3 (20 mins)	0.2292	0.1801
Al_2O_3 (25 mins)	0.2312	01819
Al_2O_3 (30 mins)	0.2347	0.1959
Al_2O_3 (35 mins)	0.24-0.30	0.15-0.30

6.4

Conclusions:

The proposed study was undertaken for comparing the properties (purity, structure and morphology) of alumina powder prepared by two different techniques. Although auto combustion method has an added advantage in obtaining the thermodynamically stable α-phase of 3N pure nano-alumina at much lower temperature, this technique is not cost effective due to the high cost of pure raw materials used. On the other hand, if we compare the particle size of the obtained alumina powder, combustion proves to be a better method for obtaining lesser particle size and low agglomeration which is a good property in substrate making. Also, if we compare the LIBS properties of the alumina powders prepared by both the methods, combustion method gives the better properties like minimum traces of impurities. In thermal conductivity and thermal diffusivity properties, the alumina powder prepared by combustion proves to give better thermal properties as required during the substrate making in LED fabrication techniques. Hence, on comparing both the methods of pure alumina (3N) preparation, auto combustion method proves to be a simple, one step, easy and useful for alumina powder preparation during the substrate making. This method does not require any post preparation annealing or sintering heat treatments to give phase pure and thermodynamically inert α-phase which resembles the actual corundum structure of the pure alumina (3N) powder.

6.5 Acknowledgements:

The authors thank Dr. A. Agnihotri, Director for his constant encouragement, laboratory facilities of XRD, SEM, TGA and permission for publishing the R&D work carried out at JNARDDC laboratory, Nagpur.

6.6 References:

1. L. D. Hart, *Alumina Chemicals: Science and Technology Handbook*, American Ceramic Society, Columbus, Ohio, USA, 1990.
2. A. Laachachi, M. Ferriol, M. Cochez, J.-M. Lopez Cuesta, and D. Ruch, "A comparison of the role of boehmite (AlOOH) and alumina (Al_2O_3) in the thermal stability and flammability of poly (methyl methacrylate)," *Polymer Degradation and Stability*, vol. 94, no. 9, pp. 1373–1378, 2009.
3. I. Lukić, J. Krstić, D. Jovanović, and D. Skala, "Alumina/silica supported K_2CO_3 as a catalyst for biodiesel synthesis from sunflower oil," *Bioresource Technology*, vol. 100, no. 20, pp. 4690–4696, 2009.
4. M. Touzin, D. Goeuriot, C. Guerret-Piécourt, D. Juvé, and H. J. Fitting, "Alumina based ceramics for high-voltage insulation," *Vacuum*, vol. 81, pp. 762–765, 2007.
5. A. Keyvani, M. Saremi, and M. Heydarzadeh Sohi, "Microstructural stability of zirconia-alumina composite coatings during hot corrosion test at 1050°C," *Journal of Alloys and Compounds*, vol. 506, no. 1, pp. 103–108, 2010.
6. R. Lach, K. Haberko, M. M. Bućko, M. Szumera, and G. Grabowski, "Ceramic matrix composites in the alumina/5-30vol.% YAG system," *Journal of the European Ceramic Society*, vol. 31, no. 10, pp. 1889–1895, 2011.
7. Cawley JD (1994) Material Science and Technology, vol.11. Volume Editor Swain M, VCH Publishers Inc, New York. p 85
8. Blendell JE, Bowen HK, Coble RL (1984) high purity alumina by controlled precipitation from aluminum sulfate solution, Amer. Cerm. Soc. 63, 797
9. Everest DA, Soycee IG, Selton B (1071) Preparation of ultrafine alumina powders by plasma evaporation, J Mat. Sci 6, 218-224
10. Ogihara T, Nakajima H, Yanaguwa H, Ogata N, Yoshida K (1991) Preparation of Monodisperse, Spherical Alumina powders from Alkoxides, J Am Ceram Soc 74, 2263-2269.
11. Du Y, Inman D (1996), Precipitation of finely divided Al_2O_3 powders by a molten salt method J Mater Chem 6, 1239-1240
12. Dawson W J, (1988) Hydrothermal Synthesis of Advanced Ceramic Powder, Journal of the American Ceramic Society Bulletin, 67, 1673-1678.
13. Alireza A, Alireza BM, Shahram B, (2010) Solvothermal synthesis, characterization and optical properties of ZnO and ZnO–Al2O3 mixed oxide nanoparticles, 405, 3585-3589.
14. Tok AIY, Boey FYC, Zhao XL (2006) Novel Synthesis of Al_2O_3 nanoparticles by flame spray pyrolysis. J Mater Process Technol178: 270-273.
15. Laine RM, Marchal JC, Sun HP, Pan XQ (2006) Nano-alpha-Al_2O_3 by liquid-feed flame spray pyrolysis. Nature Mater 5: 710-712.
16. Granado S, Ragel V, Cabanas V, San Roman J,Vallet-Regi M (1997) Influence of □-Al_2O_3 morphology and particle size on drug release from ceramic/polimer composites. J Mater Chem 7: 1581-1585.
17. Kim SM, Lee YJ, Jun KW, Park JY, Potdar HS (2007) Synthesis of thermo-stable high surface area alumina powder from sol-gel derived boehmite. Mater Chem Phys 104: 56-61.
18. Tadanaga K, Yamaguchi N, Uraoka Y, Matsuda A, Minami T, Tatsumisago M (2008) Anti-reflective properties of nano-structured alumina thin films on poly (methyl methacrylate) substrates by the sol-gel process with hot water treatment. Thin Solid Films 516: 4526-4529.

19. Yamaguchi A, Hotta K, Teramae N (2009) Optical waveguide sensor based on a porous anodic alumina/aluminum multilayer film. Anal Chem 81: 105-111.
20. Kim SH, Kim, CE, Oh YJ (1997) Influence of Al_2O_3 buffer layer on the crystalline structure and dielectric property of $PbTiO_3$ thin film by sol-gel processing. J Mater Sci Lett 16: 257-259.
21. Levin I, Brandon D (1998) Metastable alumina polymorphs: Crystal structures and transition sequences.J Am Ceram Soc 81: 1995-2012.
22. Santos PS, Santos HS, Toledo SP (2000) Standard transition aluminas: Electron microscopy studies.J Mater Res 3, 104-114.
23. Zeng WM, Rabelo AA, Tomasi R (2001) Synthesis of □-Al_2O_3 nanopowder by sol-freeze drying method. Key Eng Mater189, 16-20.
24. Madhu Kumar P, Balasubramanian C, Sali ND, Bhoraskar SV, Rohatgi VB, Badrinarayanan S (1999) Nanophase alumina synthesis in thermal arc plasma and characterization: correlation to gas-phase studies. Mater Sci Eng B 63, 215-227.
25. Popp U, Herbig R, Michel G, Muller E, Oestreich Ch (1998) Properties of nanocrystalline ceramic powders prepared by laser evaporation and recondensation. J Eur Ceram Soc18, 1153-1160.
26. Pang Y, Bao X (2002) Aluminium oxide nanoparticles prepared by water-in-oil emulsions. J Mater Chem 12, 3699-3704.
27. Deng SG, Lin YS (1997) Microwave synthesis of mesoporous and microporous alumina powders. J Mater Sci Lett 16, 1291-1294.
28. Roy R (1987) Ceramics by the solution-sol-gel route. Science 238, 1664-1669.
29. Bahlawane N, Watanabe T (2000) New sol-gel route for the preparation of pure □-alumina at 950^{o}C. J Am Ceram Soc 83, 2324-2326.
30. Aghababazadeh R, Mirhabibi AR, PourasadJ, Brown A, Brydson R, Banijamali S, Mahabad N (2007) Economical synthesis of nanocrystalline alumina using an environmentally low-cost binder. Surface Sci 601, 2864-2867.
31. Bhaduri S, Zhou E, Bhaduri SB (1996) Auto ignition processing of nanocrystalline □-Al_2O_3. Nanostruct Mater 7, 487-496.
32. Kaya C, He JY, Gu X, Butler EG (2002) Nanostructured ceramic powders by hydrothermal synthesis and their applications. Microporous Mesoporous Mater 54, 37-49.
33. J.J. Kingsley, K. Suresh, K.C. Patil, Combustion synthesis of fine-particle metal aluminates, J. Mater. Sci. 25 (1990) 1305e1312.
34. J.J. Kingsley, N. Manickam, K.C. Patil, Combustion synthesis and properties of fine particle fluorescent aluminous oxides, Bull. Mater. Sci. 13 (1990) 179e189.
35. Sharma A, Rani A, Singh A, Modi OP, Gupta GK (2014) Synthesis of alumina powder by the urea-glycine-nitrate combustion process: a mixed fuel approach to nanoscale metal oxides. Appl Nanosci 4, 315-323.
36. Khorrami SA, Ahmad MB, Lotfi R, Shameli K, Sedaghat S, Shabanzadeh P, Baghchesara MA (2012) Preparation of gamma-Al_2O_3 nanocrystallites by sol-gel auto combustion process and production of Al-Al_2O_3 aluminium matrix composites. Dig J Nanomater Bios 7, 871-876.
37. Rajaeiyan A, Bagheri-Mohagheghi MM (2013) Comparison of urea and citric acid complexing agents and annealing temperature effect on the structural properties of □- and □- alumina nanoparticles synthesized by sol-gel method. Hindawi Publishing Corporation, Advances in Material Science & Engineering 2013: Article ID 791641, 9 pages.

38. Roque-Ruiz JH, Reyes-Lopez SY (2016) Synthesis of □-Al_2O_3nanopowders at low temperature from aluminum formate by combustion process. J Mater SciEng 6, 1000305.
39. Fujiwara S, Tamura Y, Maki H, Azuma N, Takeuchi Y (2007) Development of new high-purity alumina. R&D Report, "SUMITOMO KAGAKU", Vol. I.
40. Kumagai M, Messing GL (1984) Enhanced densification of boehmite sol-gels by □-alumina seeding. J Am Ceram Soc 67, c230-c231.
41. Kumagai M, Messing GL (1985) Controlled transformation and sintering of a boehmite sol-gel by □-alumina seeding. J Am Ceram Soc 68, 500-505.
42. McArdle JL, Messing GL (1993) Transformation, microstructure development, and densification in □-Fe_2O_3- seeded boehmite-derived alumina. J Am Ceram Soc 76, 214-222.
43. Burtin P, Brunelle JP, Pijolat M, Soustelle M (1987) Influence of surface area and additives on the thermal stability of transition alumina catalyst supports. I: Kinetic data. Appl Catal, 34, 225-238.

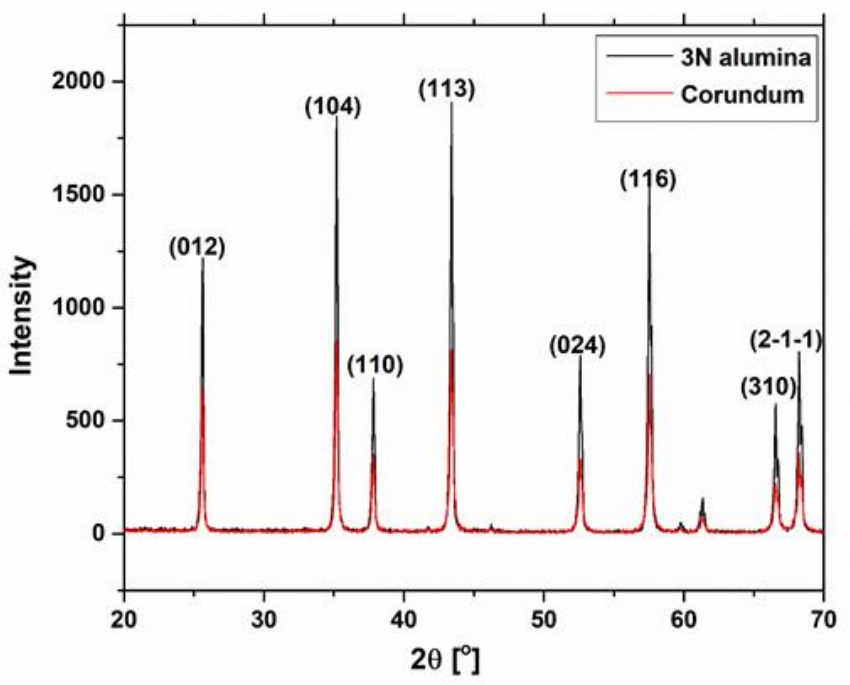

Figure 6.1: XRD Pattern of As Prepared Nano-Alumina by SGAC Method, Compared with Standard Calculated Data

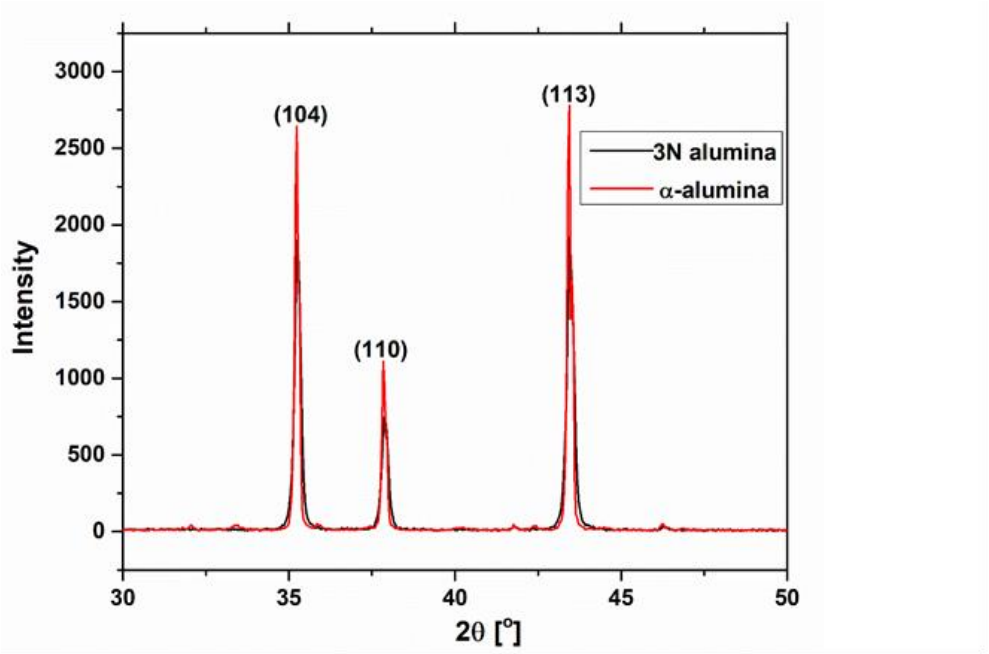

Figure 6.2: XRD Pattern of As Prepared Nano-Alumina by Alkoxide Method Compared with Standard Calculated Data

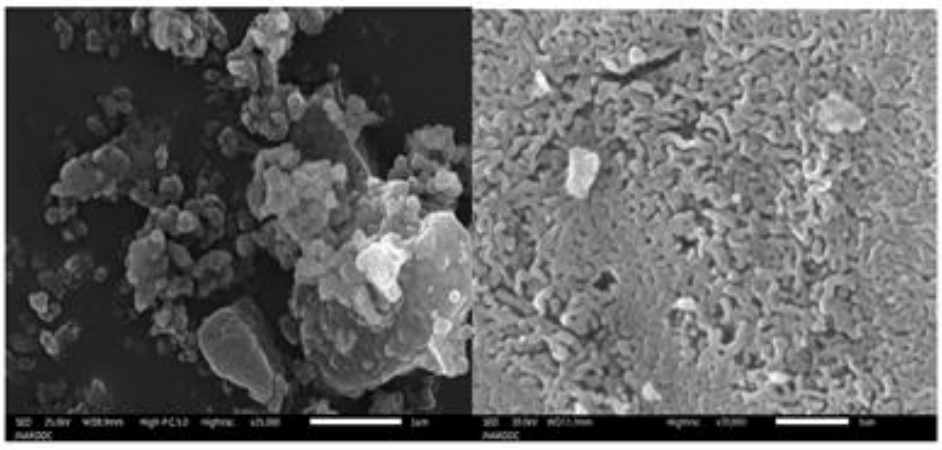

Figure 6.3: SEM Micrographs of

(a) Alumina Prepared by Sol Gel Auto Combustion and

(b) Alumina Prepared by Alkoxide Route

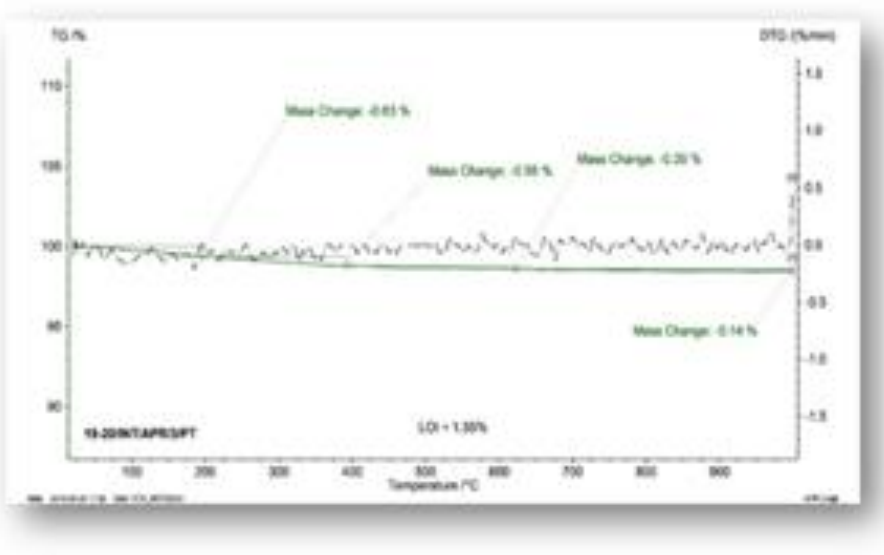

Figure 6.4: TG thermograph of Alumina Powder Prepared by Combustion Method

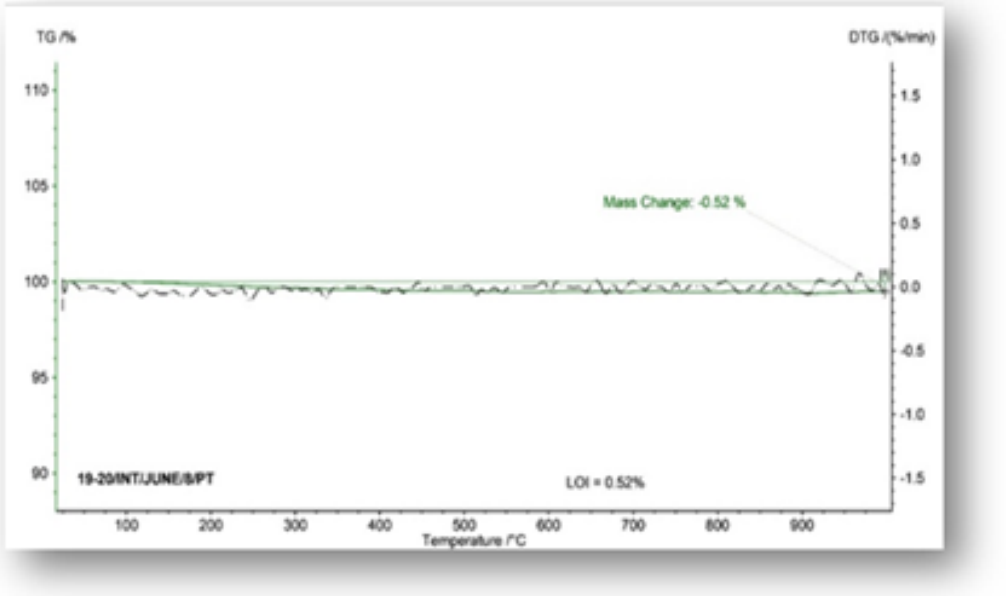

Figure 6.5: TG Thermograph of Alumina Powder Prepared by Alkoxide Method

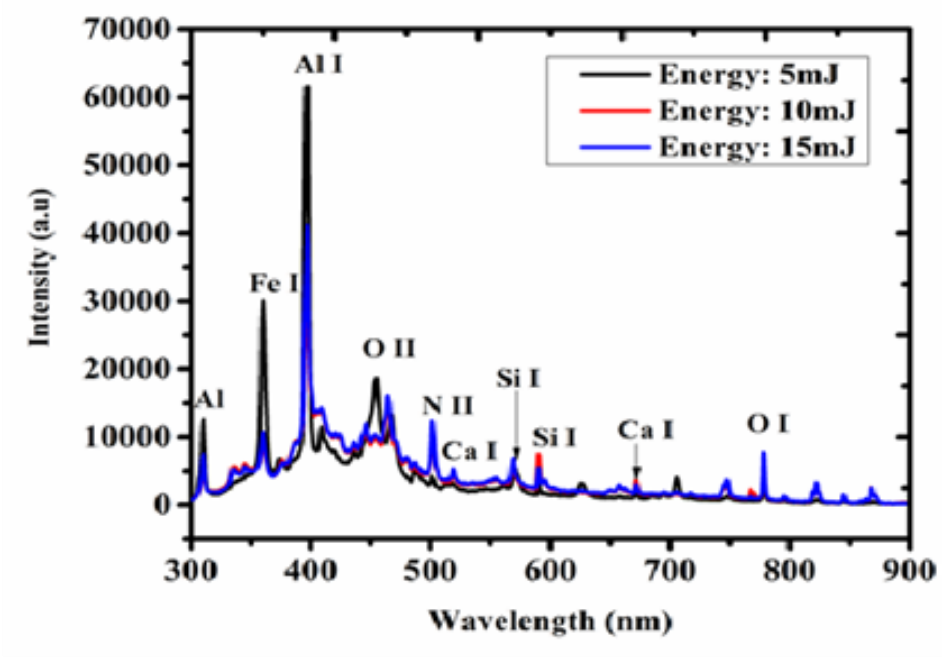

Figure 6.6: Laser Induced Breakdown Spectra of Alumina at Different Energy Levels

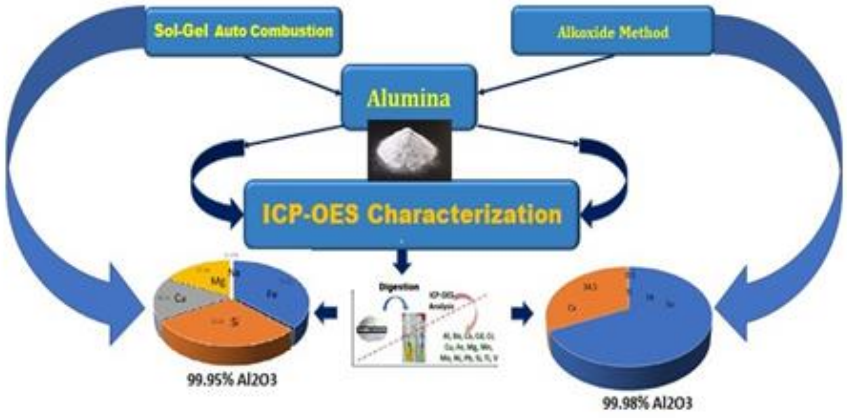

Graphical Abstract